

Decomposition of Organic Compounds over NaBiO₃ under Visible Light Irradiation

Tetsuya Kako,[†] Zhigang Zou,[‡] Masahiko Katagiri,[§] and Jinhua Ye^{*†}

Photocatalytic Materials Center, National Institute for Materials Science (NIMS), 1-2-1 Sengen, Tsukuba, Ibaraki 305-0047, Japan, Ecomaterials and Renewable Energy Research Center (ERERC), Nanjing University, 22 Hankou Road, Nanjing 210093, China, and Computational Materials Science Center (CMSC), National Institute for Materials Science (NIMS), 1-2-1 Sengen, Tsukuba, Ibaraki 305-0047, Japan

Received May 14, 2006. Revised Manuscript Received November 15, 2006

We investigated photophysical and photooxidation properties of NaBiO₃ containing Bi (V) for the first time. The optical absorption of NaBiO₃ was characterized by the sharp decrease at about 470 nm followed by the long tail up to 600 nm. The photooxidation activity evaluated from the decomposition of gaseous 2-propanol and methylene blue (MB) dye in the liquid phase revealed that NaBiO₃ is a prominent material for photooxidation of organics in the range of visible light. In addition, we calculated the electronic structures of bulk NaBiO₃ in the framework of density functional theory (DFT). As a result, strong dispersion from the hybridized Na 3s and O 2p orbitals that was identified at the bottom of the conduction band (CB) was considered to contribute to the high activity of this material.

1. Introduction

Recently, photocatalytic reactions on semiconductors have been utilized for many applications, such as air cleaners, self-cleaning materials, and antibacterial materials.^{1–3} The reactions are generally recognized as phenomena originating from electrons and holes excited by absorption of photons with energy larger than the band gap of semiconductors. The holes have a strong potential to draw electrons out of organic and inorganic contaminants, resulting in decomposition of hazardous materials, such as harmful gases, oil, and bacteria.^{4–8}

Titanium dioxide (TiO₂) is the most widely used photocatalyst among semiconductors. TiO₂ photocatalysis is active under ultraviolet (UV) light irradiation, but not active under irradiation of visible light, which is the main component in solar light and indoor illuminations. For this reason, TiO₂ is not suitable for indoor use because of insufficient supply of UV light. Therefore, a lot of work has been done to develop visible-light-sensitive photocatalysts. One of the efforts in the development is modification of TiO₂ by doping with

metallic or nonmetallic elements such as V and Cr^{9–11} or N, S, and C.^{12–17} Another challenge is to develop new materials.^{18–23} Especially, Bi(III)-containing oxides such as BiVO₄ and Bi₂WO₆ have been reported to be promising photocatalysts under visible light irradiation.^{18–21} As well as Bi(III)-containing oxides, Bi(V)-containing oxides are also interesting materials as the candidates of visible-light-sensitive oxides. In fact, some Bi (V)-containing oxides are yellow or brown, which shows the absorption of visible light. To the best of our knowledge, the photooxidation activity of Bi(V)-containing oxides has not been reported yet, except for the report about O₂ production from AgNO₃ solution over Ba₂Bi(III)Bi(V)O₆ under visible light irradiation.²⁴ It is unclear whether the origin of visible-light-sensitivity of Ba₂Bi(III)Bi(V)O₆ is due to Bi(III) or the mixed-valence state of Bi(III) and Bi(V).

* Corresponding author. E-mail: Jinhua.Ye@nims.go.jp.

[†] Photocatalytic Materials Center, NIMS.

[‡] Nanjing University.

[§] Computational Materials Science Center, NIMS.

- (1) A. Fujishima, A.; Hashimoto, K.; Watanabe, T. *TiO₂ Photocatalysis Fundamentals and Applications*; BKC Inc: Tokyo, 1999.
- (2) Ollis, D. F.; Al-Ekabi, H. *Photocatalytic Purification and Treatment of Water and Air*; Elsevier: Amsterdam, 1993.
- (3) Hoffmann, M. R.; Martin, S. T.; Choi, W. Y.; Bahnemann, D. W. *Chem. Rev.* **1995**, *95*, 69.
- (4) Panayotov, D.; Kondratyuk, P.; Yates, J. T., Jr. *Langmuir* **2004**, *20*, 3674.
- (5) Negishi, N.; Takeuchi, K.; Ibusuki, T. *J. Mater. Sci.* **1998**, *33*, 5789.
- (6) Kako, T.; Nakajima, A.; Watanabe, T.; Hashimoto, K. *Res. Chem. Intermed.* **2005**, *31*, 371.
- (7) Kako, T.; Irie, H.; Hashimoto, K. *J. Photochem. Photobiol., A* **2005**, *171*, 131.
- (8) Sunada, K.; Watanabe, T.; Hashimoto, K. *J. Photochem. Photobiol., A* **2003**, *156*, 227.

- (9) Borgarello, E.; Kiwi, J.; Gratzel, M.; Pelizzetti, E.; Visca, M. *J. Am. Chem. Soc.* **1982**, *104*, 2996.
- (10) Serpone, N.; Lawless, D.; Disdier, J.; Herrmann, J. M. *Langmuir* **1994**, *10*, 643.
- (11) Yamashita, H.; Harada, M.; Misaka, J.; Takeuchi, M.; Ikeue, K.; Anpo, M. *J. Photochem. Photobiol., A* **2002**, *148*, 257.
- (12) Asahi, R.; Morikawa, T.; Ohwaki, T.; Aoki, K.; Taga, Y. *Science* **2001**, *293*, 269.
- (13) Irie, H.; Watanabe, Y.; Hashimoto, K. *J. Phys. Chem. B* **2003**, *107*, 5483.
- (14) Ohno, T.; Mitsui, T.; Matsumura, M. *Chem. Lett.* **2003**, *32*, 364.
- (15) Irie, H.; Watanabe, Y.; Hashimoto, K. *Chem. Lett.* **2003**, *32*, 772.
- (16) Liu, H. Y.; Gao, L. *Chem. Lett.* **2004**, *33*, 730.
- (17) Kasahara, A.; Nukumizu, K.; Hitoki, G.; Takata, T.; Kondo, J. N.; Hara, M.; Kobayashi, H.; Domen, K. *J. Phys. Chem. A* **2002**, *106*, 6750.
- (18) Kudo, A.; Omori, K.; Kato, H. *J. Am. Chem. Soc.* **1999**, *121*, 11459.
- (19) Kudo, A. *J. Ceram. Soc. Jpn* **2001**, *109*, S81.
- (20) Tang, J. W.; Zou, Z. G.; Ye, J. H. *Catal. Lett.* **2004**, *92*, 53.
- (21) Kako, T.; Ye, J. H. *Mater. Trans.* **2005**, *46*, 2694.
- (22) Kato, H.; Kobayashi, H.; Kudo, A. *J. Phys. Chem. B* **2002**, *106*, 12441.
- (23) Kim, H. G.; Hwang, D. W.; Lee, J. S. *J. Am. Chem. Soc.* **2004**, *126*, 8912.
- (24) Li, Z. S.; Xu, N.; Chen, Y. F.; Zou, Z. G. *Res. Chem. Intermed.* **2005**, *31*, 529.

Thus, we studied the photophysical and photooxidation properties of NaBiO₃ as the oxide containing Bi(V) only. As a result, we found that NaBiO₃ shows high activity for MB bleaching under visible light irradiation.

2. Experimental Section

The NaBiO₃ sample was prepared by heating commercial NaBiO₃·*n*H₂O, which was purchased from Wako Pure Chemicals Industries Ltd., in air at 413 K for 5 h. Crystal structures and optical absorption spectra were investigated with an X-ray diffractometer (JDX-3500; JEOL, Japan) using Cu K α radiation and with a UV–vis diffuse reflectance spectrophotometer (UV-2500PC; Shimadzu Corp., Japan), respectively.

The photooxidation activity of NaBiO₃ was evaluated from two kinds of reactions. One reaction was decomposition of gaseous 2-propanol into acetone. The other was bleaching of MB dye solvated in water. These reactions are recognized as the most standard ones for the evaluation of photooxidation activity.^{12–16,25–31} In the decomposition of 2-propanol, we investigated the relationship between the photooxidation activity and cutoff wavelength of irradiated light at room temperature. The powder of 0.4 g of NaBiO₃ was spread uniformly over a 5.7 cm² area and set in a reactor of a 500 mL closed glass vessel. The atmosphere in the reactor was replaced by synthetic air, and subsequently, air-based mixed gas containing 2-propanol was introduced into the reactor. By this operation, the concentration of 2-propanol was ca. 600 ppm inside the reactor. The reactor was then kept in the dark until an equilibrium adsorption state was confirmed. After confirming the state, the reactor was irradiated with visible light, which was emitted by a Xe arc lamp through a sharp cutoff filter (L-42, Y-44, Y-48, Y-50, O-54, R-60, and R-64; Hoya Corp., Japan) and a water filter for cutting off IR (infrared). The cutoff wavelength of irradiated light was controlled using these sharp cutoff filters. The light intensity was measured with a spectroradiometer (USR-40D; Ushio Corp., Japan). The 2-propanol and acetone concentrations were measured using a gas chromatograph (GC-14B; Shimadzu) equipped with a flame-ionized detector.

In a bleaching test of MB, the powder of 0.3 g of NaBiO₃ was suspended in 100 mL of MB solution (pH ~6) with the initial concentration of 16 mg L⁻¹ in a glass reactor with a 44 cm² cross-section and 5 cm height. To obtain the equilibrium adsorption states, we kept the suspension in the dark for 90 min with agitation, prior to visible light irradiation. The reactor was then irradiated with visible light emitted by a 300 W Xe arc lamp with a UV cutoff filter (L-42; Hoya). In the measurement of MB concentration, the slurry samples including NaBiO₃ and MB solution were separated by a syringe equipped with a membrane filter unit (Millex; Millipore Corp., United States). The MB concentration was determined by measuring the maximum absorbance around $\lambda = 663$ nm as a function of irradiation time in the separated MB solution with a UV–vis spectrophotometer (Shimadzu).

For comparison, N-doped anatase TiO₂ and BiVO₄ with a monoclinic sheelite structure were utilized as references of visible-

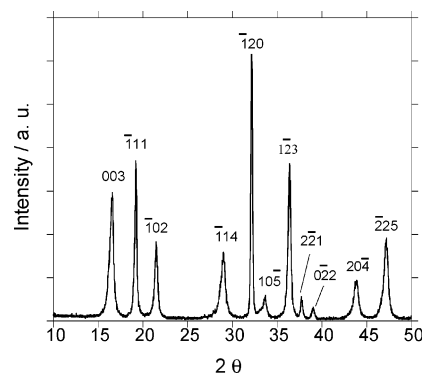


Figure 1. X-ray diffraction pattern of NaBiO₃.

light-driven photocatalysts. N-doped TiO₂ was prepared by heating commercially available TiO₂ (ST-01; Ishihara Sangyo Kaisha Ltd., Japan) under NH₃ gas flow at 873 K for 3 h.^{12,13} BiVO₄ was prepared in an aqueous medium by the method reported by Kohtani et al.³² The specific surface areas of NaBiO₃, N-doped TiO₂, and BiVO₄, measured using a BET (Brunnauer–Emmett–Teller) surface area analyzer (Gemini 2360; Micromeritics Corp., United States), were estimated to be 5.0, 43, and 1.2 m² g⁻¹, respectively.

The durability of the NaBiO₃ photooxidation activity was also evaluated using repeated experiments of MB bleaching. In this experiment, the MB concentration of the reacted solution was measured every 6 min. In the beginning of each experimental circle, MB solution was injected into the reactor to compensate for the decrease in the amount and concentration of MB solution caused by former measurements. By this operation, the concentration and the total volume of the solution were adjusted to 12 mg L⁻¹ and 100 mL, respectively, for each repeated experiment.

The plane-wave-based density functional theory (DFT) calculation of NaBiO₃ was performed with the CASTEP program.³³ The core electrons were replaced by the Vanderbilt ultra-soft pseudo-potentials.³⁴

3. Results and Discussion

3.1. Crystal Structure. Figure 1 shows the X-ray diffraction pattern of the prepared sample. After heating NaBiO₃·*n*H₂O at 413 K, we identified its XRD pattern with that of the dehydrated phase, NaBiO₃.^{35,36} This NaBiO₃ is well-crystallized into an ilmenite structure (space group $R\bar{3}$) with lattice parameters $a = 5.564$ Å, $c = 15.99$ Å, $\gamma = 120^\circ$. A schematic illustration of the crystal structure of NaBiO₃ is shown in Figure 2. BiO₆ octahedral layers are sandwiched in between NaO₆ octahedral layers along the *c*-axis.

3.2. Optical Property. Prior to evaluation of the photooxidation activity, the optical absorption spectrum of NaBiO₃ was measured, as shown in Figure 3. The NaBiO₃ spectrum was characterized by the sharp decrease around 470 nm due to the band gap transition and the long tail up to about 700

(25) Tang, J. W.; Zou, Z. G.; Ye, J. H. *Angew. Chem., Int. Ed.* **2004**, *43*, 4463.

(26) Ihara, T.; Miyoshi, M.; Ando, M.; Sugihara, S.; Iriyama, Y. *J. Mater. Sci.* **2001**, *36*, 4201.

(27) Kako, T.; Zou, Z.; Ye, J. *Res. Chem. Inter.* **2005**, *31*, 359.

(28) Ohko, Y.; Hashimoto, K.; Fujishima, A. *J. Phys. Chem. A* **1997**, *101*, 8057.

(29) Moriguchi, I.; Orishikida, K.; Tokuyama, Y.; Watabe, H.; Kagawa, S.; Teraoka, Y. *Chem. Mater.* **2001**, *13*, 2430.

(30) Song, K. Y.; Park, M. K.; Kwon, Y. T.; Lee, H. W.; Chung, W. J.; Lee, W. I. *Chem. Mater.* **2001**, *13*, 2349.

(31) Ohko, Y.; Fujishima, A.; Hashimoto, K. *J. Phys. Chem. B* **1998**, *102*, 1724.

(32) Kohtani, S.; Makino, S.; Kudo, A.; Tokumura, K.; Ishigaki, Y.; Matsunaga, T.; Nikaido, O.; Hayakawa, K.; Nakagaiki, R. *Chem. Lett.* **2002**, 660.

(33) Payne, M. C.; Teter, M. P.; Allan, D. C.; Arias, T. A.; Joannopoulos, J. D. *Rev. Mod. Phys.* **1992**, *64*, 1045.

(34) Vanderbilt, D. *Phys. Rev. B* **1990**, *41*, 7892.

(35) International Centre for Diffraction Data. *Powder Diffraction File*; McClune, W. F., Mrose, M. E., Post, B., Weissmann, S., McMurdie, H. F., Eds.; JCPDS International Centre for Diffraction Data: Swarthmore, PA, 1987; Inorganic Vols. 29–30, p 957.

(36) Kumada, N.; Kinomura, N.; Sleight, A. W. *Mater. Res. Bull.* **2000**, *35*, 2397.

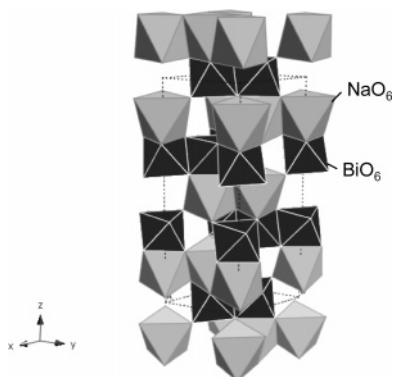


Figure 2. Crystal structure of NaBiO₃.

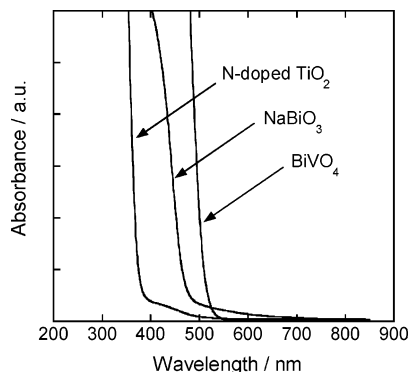


Figure 3. Optical absorption spectra of NaBiO₃, N-doped TiO₂, and BiVO₄.

nm, which is probably caused by the lattice defects, such as oxygen vacancies. The optical band gap was estimated to be about 2.6 eV from the onset of the absorption edge. The band gap of Bi(V)-containing oxides, such as MgBi₂O₆ (1.8 eV)³⁷ and NaBiO₃ (2.6 eV), is apt to be smaller than that of Bi(III)-containing oxides, such as Bi₂O₃ (2.8–2.9 eV),³⁸ Bi₂WO₆ (2.8 eV), and Bi₂W₂O₉ (3.0 eV).¹⁹ On the other hand, the band gap of BiVO₄ is estimated to be 2.3 eV and is smaller than that of the other reported Bi(III)-containing photocatalysts. Because BiVO₄ can absorb a larger amount of visible light than NaBiO₃, BiVO₄ is considered to be a suitable photocatalyst for comparison of the activity of a Bi(III)-containing oxide with that of a Bi(V)-containing oxide.

The spectrum of the reference photocatalyst, the N-doped TiO₂ was measured and shown in Figure 3. The spectrum was quite similar to that of the 0.5% N-doped TiO₂, of which relatively high activity was reported by Irie et al.¹³ As predicted from its pale yellow color, the N-doped TiO₂ could also absorb visible light up to ca. 550 nm in wavelength. However, compared to NaBiO₃, the absorbance of N-doped TiO₂ was obviously weaker in the longer visible light region.

3.3. Band Structure. The electronic structure was calculated using the plane-wave-based density functional method. Figure 4 shows the density of states (DOS) of bulk NaBiO₃. The highest occupied band corresponding to the broad valence band (VB) was found to be mainly composed of the O 2p orbital. Because of the empty Bi 6s orbitals, the

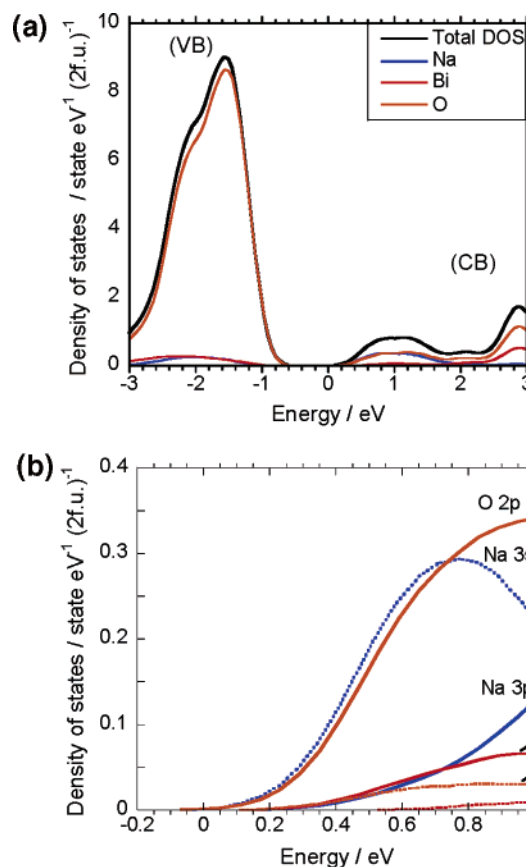


Figure 4. (a) Total and partial DOS of NaBiO₃. (b) Partial DOS of NaBiO₃ around the bottom of the conduction band.

contribution of Bi 6s to the VB seems to be much smaller than that in the oxides containing Bi³⁺ whose valence electron is Bi 6s. Therefore, the proposed band structure of VB in NaBiO₃ is different from that of Bi(III)-containing oxides such as CaBi₂O₄, which is composed of hybridized orbitals between Bi 6s and O 2p at the top of VB.²⁵ We also found that the bottom of the CB in NaBiO₃ is composed of the hybridized Na 3s and O 2p orbitals (see Figure 4b). This result is obviously different from the Bi 6p orbital contributing mainly at the bottom of the CB in Bi³⁺-containing oxides. A large dispersion was observed in the hybridized sp orbitals in the CB of NaBiO₃, suggesting that the photoexcited electrons have high mobility on the sp bands. This may lead to suppression of the recombination of electron–hole pair and a relatively higher photooxidation activity of the material than that of a Bi(III)-containing oxide. Further works on evaluation of the charge mobility of these oxides and examination of the relationship between the activities and the charge mobility of Bi(III)- and Bi(V)-containing oxides are in progress.

3.4. Photooxidation Activity. We conducted experiments to evaluate the photooxidation activity of NaBiO₃ in decomposing 2-propanol and MB. Figure 5 shows the cutoff wavelength dependence of irradiated light intensity and evolved acetone concentration for 1 h light irradiation in the decomposition process of 2-propanol. The intensity decreased gradually as the cutoff wavelength increased because most of the light below the cutoff wavelength was eliminated by the cutoff filters. At irradiation time less than 1 h, there was no CO₂ or other intermediates except for acetone detectable

(37) Mizoguchi, H.; Bhuvanesh, N. S. P.; Woodward, P. M. *Chem. Commun.* **2003**, 1084.

(38) Maruthamuthu, P.; Gurusathan, K.; Subramanian, E.; Sastri, M. V. *C. Int. J. Hydrogen Energy* **1993**, *18*, 9.

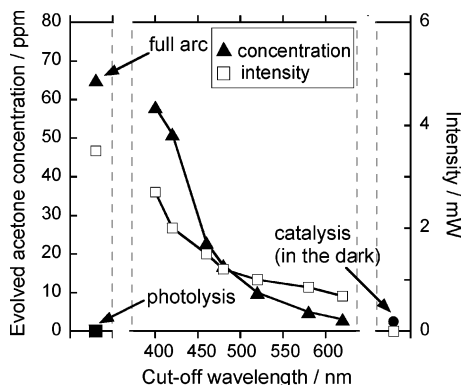


Figure 5. Cutoff wavelength dependence of irradiated light intensity and evolved acetone concentration for 1 h through decomposition of 2-propanol on NaBiO₃. Closed square, photolysis; closed circle, catalysis.

in the gas phase. Therefore, the photooxidation activity was evaluated from the concentration of evolved acetone at the initial stage. Similar evaluations were applied for photocatalytic activity over TiO₂.^{28,31}

As shown in Figure 5, NaBiO₃ showed a high photooxidation activity of 65 ppm h⁻¹ under full arc irradiation. With an increase in the wavelength of cutoff filters applied, the activity decreased quickly, in accordance with the decrease in the irradiated light intensity. At around 460 nm, a significant decrease in the photooxidation activity of NaBiO₃ was observed, which nearly corresponded to the onset of absorption edge. This may be because the photooxidation under light longer than 460 nm is derived from lattice defects. To clarify the effect of catalysis and photolysis, we also carried out the decomposition experiments in the dark with NaBiO₃ (catalysis) and under full arc light irradiation without NaBiO₃ (photolysis). Part of the 2-propanol was decomposed in the dark, but decomposition by photolysis was hardly observed. The concentration of evolved acetone in these two conditions was lower than those in the decomposition over the photocatalyst, even under the light irradiation with the 620 nm cutoff wavelength. This suggests that the evolution of acetone was largely caused by NaBiO₃ photooxidation. From these results, it is obvious that this oxide is a visible light sensitive oxide.

Figure 6 shows the decrease in MB concentration in the NaBiO₃-suspended solution as a function of reaction time. As comparison, the results of MB decomposition over N-doped TiO₂ and BiVO₄ under visible light irradiation are also given in Figure 6. Prior to light irradiation, the solution was kept in the dark for 90 min to obtain equilibrium adsorption states. At this stage, MB concentration in the solutions changed from 16 to 10 mg L⁻¹ in the NaBiO₃ system (Figure 6d), 12 mg L⁻¹ in the N-doped TiO₂ one, and 14 mg L⁻¹ in the BiVO₄ system. This result suggests that NaBiO₃ had a higher adsorption ability for MB. We then applied visible light to the reactor. For only 10 min of visible light irradiation, MB was completely bleached with the outstanding rate by NaBiO₃ (Figure 6a). Assuming that the bleaching reaction proceeded the pseudo-first-order reaction, we estimated the rates of MB decomposed over NaBiO₃ (BET, 5 m² g⁻¹), N-doped TiO₂ (BET, 43 m² g⁻¹), and BiVO₄ (BET, 1.2 m² g⁻¹) to be ca. 4.2 × 10⁻¹, 4.6 × 10⁻², and 2.9 × 10⁻² min⁻¹, respectively. Although the surface

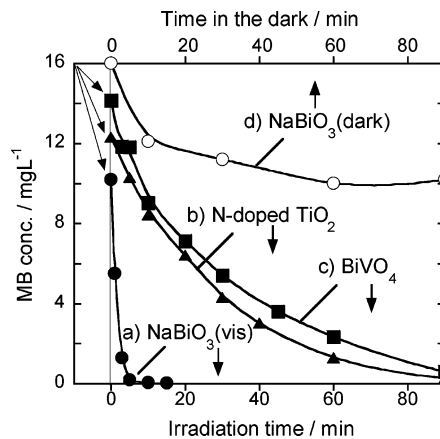


Figure 6. Time dependence of MB bleached in the dark and change in MB concentration on NaBiO₃ and N-doped TiO₂ as a function of reaction time. (a) MB concentration on NaBiO₃ under visible light irradiation, (b) MB concentration on N-doped TiO₂ under visible light irradiation, (c) MB concentration on BiVO₄ under visible light irradiation, and (d) MB concentration on NaBiO₃ in the dark.

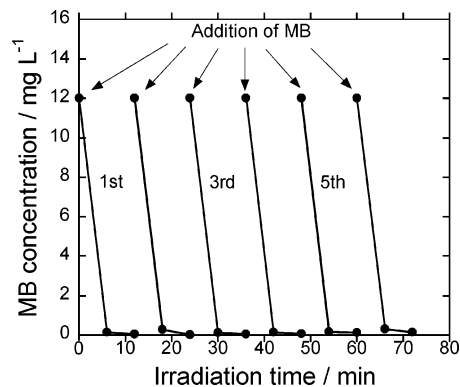


Figure 7. Evaluation of durability of NaBiO₃ photooxidation from the repeatable bleaching of MB under visible light irradiation. MB concentration in the reactor was tuned to 12 mg L⁻¹ every 12 min.

area of NaBiO₃ is about 1 order smaller than that of N-doped TiO₂, the bleaching rate over NaBiO₃ may be more than 1 order faster than that of N-doped TiO₂. Moreover, NaBiO₃ showed a higher rate than BiVO₄ and the other reported Bi(III)-containing oxides such as Bi₂O₃ and CaBi₂O₄.²⁸ This superiority may be due to the higher mobility of photo-generated electrons in NaBiO₃ and its strong adsorption property to MB. We also found that besides MB dye, other dyes such as Orange II and Rhodamine B were also quickly bleached by the NaBiO₃ photooxidation under visible light irradiation.

Figure 7 shows the results of repeated experiment for the durability of MB bleaching on NaBiO₃. MB was quickly bleached after every injection of MB, suggesting that NaBiO₃ shows relatively stable performance for MB bleaching. However, in the sixth run, the bleaching rate was slightly decreased. The decrease in the activity of MB bleaching may be due to the decrease in the photooxidation activity of NaBiO₃ and the decrease in the amount of NaBiO₃ in the reactor by sampling the slurry at every measurement of the MB concentration. After the sixth run, ca. 40% of the NaBiO₃ powder was removed by sampling. Moreover, we evaluated the XRD pattern of the sample after the sixth run (Figure 8). The XRD pattern was almost similar to that of the as-prepared sample, except for the appearance of four small

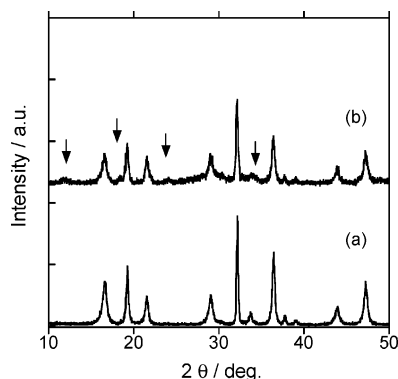


Figure 8. XRD patterns of NaBiO_3 before and after MB bleaching: (a) before reaction and (b) after the sixth run for the repeatable bleaching of MB. Arrow suggested the pattern corresponding to $\text{NaBiO}_3 \cdot 2\text{H}_2\text{O}$.

peaks corresponding to $\text{NaBiO}_3 \cdot 2\text{H}_2\text{O}$.³⁵ Judging from these results, NaBiO_3 is considered to be relatively stable to visible light under the present experimental conditions.

4. Conclusion

We investigated the photophysical properties, electronic structure, and photooxidation activity of NaBiO_3 and acquired the following results. The onset optical absorption edge was around 470 nm; from this value, the optical band gap was estimated to be about 2.6 eV. We also performed the calculation of electronic structure of NaBiO_3 ; strong dispersion from the hybridized Na 3s and O 2p orbitals was

identified at the bottom of the conduction band, whereas the flat structure of O 2p was observed at the top of the valence band. We examined the photooxidation activity, employing an example of the decomposition of 2-propanol in the gas phase and MB dye in the liquid phase under visible light irradiation. 2-Propanol was quickly decomposed under irradiation of light in a cutoff wavelength less than about 460 nm with NaBiO_3 photooxidation. However, under the irradiation of light in a longer cutoff wavelength, the activity became dramatically decreased, because this decomposition was caused by lattice defects. MB dye was easily bleached under visible light ($\lambda > 400$ nm) irradiation and the bleaching rate was faster than that over N-doped TiO_2 . These results suggested that NaBiO_3 is the prominent material for photooxidation of organics in the range of visible light. From band gap calculation, NaBiO_3 showed strong dispersion on CB. Under strong dispersion, electrons excited by irradiation possess a small effective mass. This may be relevant to the high migration mobility of carriers toward the surface, and hence high photooxidation.

Acknowledgment. The present research is supported in part by the Global Environment Research Fund and a Grant-in-Aid for Scientific Research on Priority Areas from the Ministry of Education, Culture, Sports, Science and Technology (MEXT) of the Japanese Government.

CM0611284